Preserved Charcoal as a Proxy for Wildfire Activity in Great Basin National Park

Undergraduate Research Thesis
Submitted in partial fulfillment of the requirements for graduation
with honors research distinction in Earth Sciences
in the undergraduate colleges of
The Ohio State University

By
James H. R. White
The Ohio State University
2019

Approved by

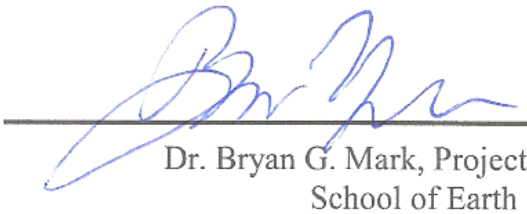

Dr. Bryan G. Mark, Project Advisor
School of Earth Sciences

Table of Contents

Abstract……..ii

Acknowledgements…….……iii

List of Figures……...…….iv

List of Tables…….……..v

Introduction…….…….1

Methods

Core Retrieval…….……..……..2

Charcoal Preparation and Counting…….…..……...……...4

Age Model Creation and Data Analysis..……...…….5

Results

Core Descriptions …….……...7

Carbon Dates……...……...……..11

Age-Depth Model…….14

Charcoal Counts……15

CharAnalysis…….16

Discussion

7,600 Calibrated Years Before Present and Older ……..18

7,600 to 5,400 Calibrated Years Before Present…….……...…….18

5,400 Calibrated Years Before Present and Younger ……..20

Recommendations for Future Work……..21

References Cited…..…….22

Appendix…….……..24

Abstract

Over the past several years, wildfire has proven to be a persistent and serious concern for the western United States. Wildfires represent complex systems where specific drivers and mechanisms may not be immediately apparent. For this reason, it is useful to look at past wildlife regimes in order to determine how human effects may induce change. This project adds to a growing body of fire research by generating a paleo-climate record of past wildfire activity within Great Basin National Park. Four sediment cores have been retrieved for this project from three different wetlands within the park. Two of these cores (extracted in 2014 and 2015) have undergone lab analysis to obtain a count of charcoal throughout each core. An age-depth model has also been constructed for each core using radiocarbon dating, allowing fire activity to be extrapolated through time. Results from this study indicate recent fire occurrence of roughly one major fire every 200 years. There appears to be an extreme period of fire activity roughly 6,800 years ago. The return interval before this point appears much longer than two hundred years, signaling a rapid, sustained shift in the ecosystem 6,800 years ago. This shift may be linked to major local scale drought events seen in other paleoclimate record around this time. Two additional cores were drilled during summer 2018 providing a clear avenue for future research. Paired with other paleo-environmental research, this analysis can be used to help understand the drivers of wildfire activity through time.

Acknowledgments

Great thanks to Bryan Mark and Jim DeGrand who have both served as incredible and understanding research mentors over these past four years. Special thanks to David Porinchu who graciously provided carbon dating services and thoughtful advice. Thanks to all the hard work of Scott Reinemann and countless other participants in the Great Basin Expeditions for collecting the cores used in this analysis. Also thank you to Julia Andreasen, Jillian Dyer, and John-Morgan Manos for their tireless lab work in service of this project. Additional thanks to Sue Welch who helped me explore other fields of research beyond my thesis. The fieldwork and analysis of this project were supported by the Western National Parks Association and graciously approved by Great Basin National Park. Additional funding has been provided by The Sharpe Innovation Seed Grant from the Department of Geography and the McKenzie Brecher Undergraduate Scholarship from the Byrd Polar and Climate Research Center. My education has been supported by the Ohio State Maximus Scholarship, the Joan Echols Scholarship from the School of Earth Sciences, the School of Earth Sciences Field Experience Travel Fund, and the Taaffe award from the Department of Geography. My personal thanks go to the NOAA Hollings Scholarship Program and everyone at the National Weather Service Fairbanks, the Alaska Fire Service, and the Alaska Center for Climate Assessment and Policy for aiding in my education and allowing me to learn many research skills critical for this project.

List of Figures

1. Drilling Location Map……..……..3
2. 2018 Drilling Rig Photo……3
3. Charcoal under Microscope Photo……5
4. DLM14 Photos……..9
5. DLM15 Photos……..10
6. SBC and SFB Photos…….13
7. Age-Depth Model……..14
8. Charcoal Counts……15
9. Charcoal Deposition Rate…….….16
10. Extrapolated Fire Frequency…….17

List of Tables

1. Carbon Dates……12

Introduction

Wildfire is an important part of the ecology within Great Basin National Park. In both high elevation forests and low elevation scrublands and grasslands, fire shapes the ecosystem. Before human occupation in the region, fire likely occurred every 10 years for lower elevation environments and every 100 years for high elevation forests (Kilpatrick et al., 2013). Human intervention has drastically reduced fire occurrence within the region leading to large scale ecologic changes (Miller et al., 2013). Climate change will probably have widespread effects on the fire ecology as well; there has already been a substantial increase in the fire season length likely due to climate change (Miller et al., 2013). In order to understand future changes, it is important to understand how the local fire regime has responded to changes in the past climate. Counting charcoal preserved in sediment cores has often been used to extrapolate fire history through time (Whitlock & Larson, 2001). Paired with other paleoclimate records such as pollen samples, charcoal analysis can be used to better understand climate mechanisms driving fire regimes. Despite the utility of such charcoal analysis, only one charcoal study has been conducted with the entire Great Basin region, and none within Great Basin National Park. (Wahl et al., 2015). Charcoal studies are commonly conducted using lake cores; the lack of lakes in fire-prone areas likely explains the lack of fire research done in this area. This thesis used meadow sediment cores from Great Basin National park in an attempt to generate a fire history for the area.

Methods

Core Retrieval

The soil core extraction sites for this project in Great Basin National Park were selected from a mixture of field reconnaissance done by Scott Reinemann and David Porinchu and wetland maps provided by park scientists. While lake cores are usually considered ideal for charcoal analysis, most lakes in the park are at elevations too high for ideal charcoal accumulation conditions due to their close proximity to the tree line. Other attempts to drill cores from lower elevation ephemeral lakes proved problematic. With these constraints, perched, seasonal wetlands within the park presented the locations most likely to have consistent deposition at lower elevations.

The first two cores of this project, DLM14 and DLM15 (drilled in 2014 and 2015 respectively), were drilled from Dead Lake Meadow (See Figure 1). Dead Lake Meadow (DLM) is situated within the Snake River catchment in the central region of the park. It lies near the ephemeral Dead Lake and contains wet, grassy vegetation surrounded by juniper and pine forest. Both cores were drilled using a modified Livingstone lake core drilling rig. This rig is human powered and has been modified to allow it to penetrate through consolidated sediment. The drill was pressed into the sediment to a maximum of 50 cm or until significant resistance was encountered. The core section was then extracted from the tube and coring continued to refusal.

Two additional cores were extracted in 2018 using a different coring method. These cores come from wet meadows further north in the park than DLM. South Fork Baker Creek (SFB) is the more southern site and is situated in the Baker Creek catchment. Strawberry Creek (SBC) is the northern most site and is situated in the Strawberry creek watershed. Both SFB and SBC are in similar but overall larger and lower elevation wetlands than the DLM site. The vegetation surrounding SFB and SBC is predominantly composed of grasses and sage with pine and juniper forest surrounding each wetland. At both SFB and SBC, a custom drilling solution was used (See Figure 2). The custom drill rig consists of a lightweight polycarbonate tube equipped with a perforated end that prevents the core from slipping out and preserves core integrity. A wooden platform clamps to the tube, allowing body weight to push the tube into the ground. Once completed, the core is pulled out in one piece using a winch system. This method produced more continuous and less compressed results than the old coring method. For transport back to the lab at Ohio State, the cores were wrapped in plastic wrap, sealed in a wooden, secured shipment crate. Once at Ohio State the cores were stored in sealed tube in a fridge cooled to 4°C to maintain moisture.

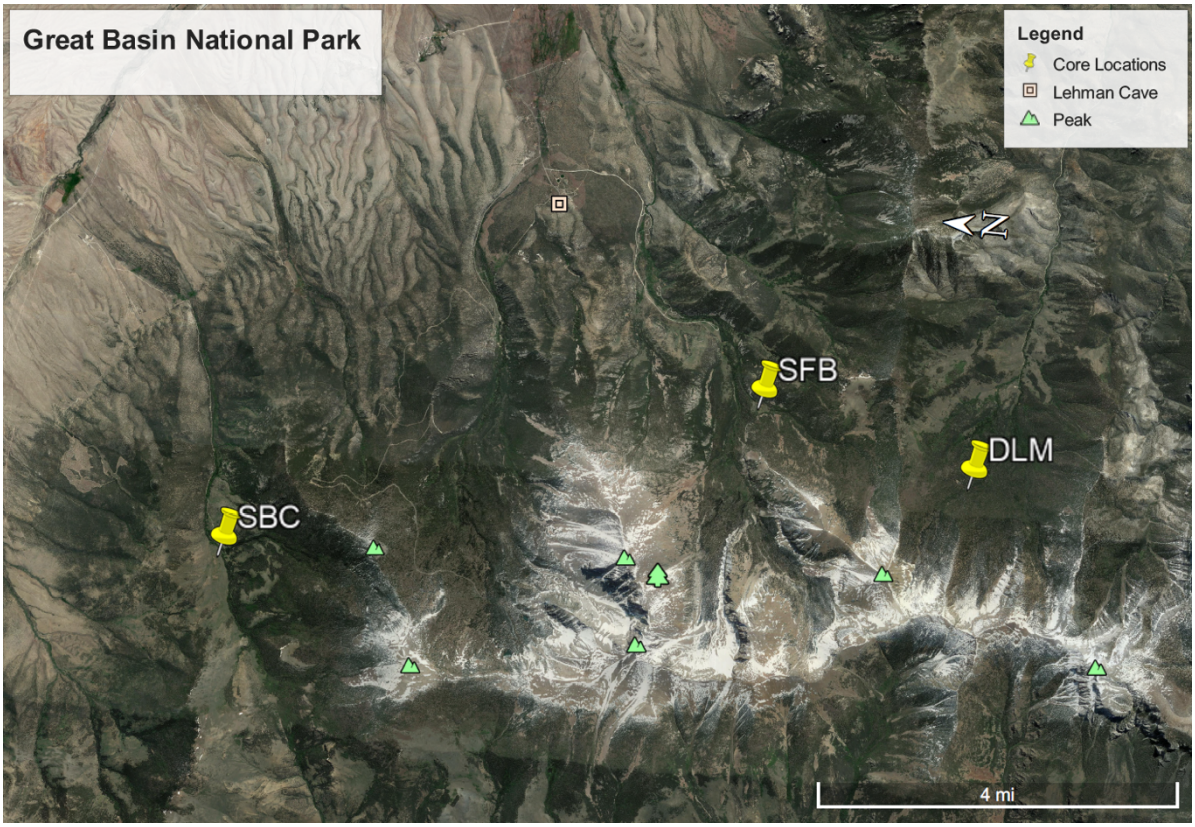

Figure 1: Map showing Great Basin National Park with the 3 main drilling sites highlighted. Lehman Caves is also shown for reference.

Figure 2: Photograph of extraction of the SFB18 core. The ring mechanism mounts onto the central tube to push it down during the drilling phase. The picture also showcases the meadow environment. (Picture credit: Bryan Mark)

Charcoal Preparation and Counting

After cores were carefully split and described in the Mercer Lab at Byrd Polar and Climate Research Center, samples were prepared for charcoal analysis following the process described by Whitlock (Whitlock & Larson, 2001). Samples of 1 cm^3 compacted sediment were carefully extracted from one side of each core at 1cm intervals (2cm intervals for DLM14). These samples were soaked individually in 10 ml of 10% sodium hexametaphosphate solution in vials that were sealed and then left to sit in the fridge at 4°C. This solution breaks up the sediment and makes it easier to sieve. After sitting in solution for at least 24 hours, 5ml of bleach was added to each vial and allowed to soak for between 5 minutes and 12 hours depending on the opacity of the sediment. The bleach increased the contrast between charcoal and other organic material. After soaking, each sediment sample was passed through 250 μm and 125 μm sieves using distilled water. Each sieve was gently washed before transferring the sediment into separate, gridded petri dishes. This process preserves macroscale charcoal while removing most aerosol-based charcoal, ensuring that a mostly local signal is preserved. The excess water in each sample was then allowed to evaporate within a closed fume hood. Once dry, the lid for each sample was sealed with electrician's tape for later analysis.

Charcoal was counted in each sample using a light microscope at a magnification power of 40x. Charcoal grains can be identified by their distinctive black coloration, angular shape, and brittle texture (Figure 3). Special care must be taken to distinguish charcoal from dark micas. Care must also be taken to avoid breaking the charcoal grains into multiple pieces. Each piece of charcoal is counted as herbaceous (burned grass or leaves), woody (burned wood), or other (different textures, often charred clay or seeds). Charcoal type was estimated using texture as described in Crawford (Crawford & Belcher, 2014). Herbaceous charcoal exhibits either a lattice like texture or bladed look where woody charcoal is most often in think chunky pieces or small splinters. This texture based method is only a best estimate and has significant likely error. After the count of each sample was completed, a selection of samples was recounted once by different researchers to ensure count consistency.

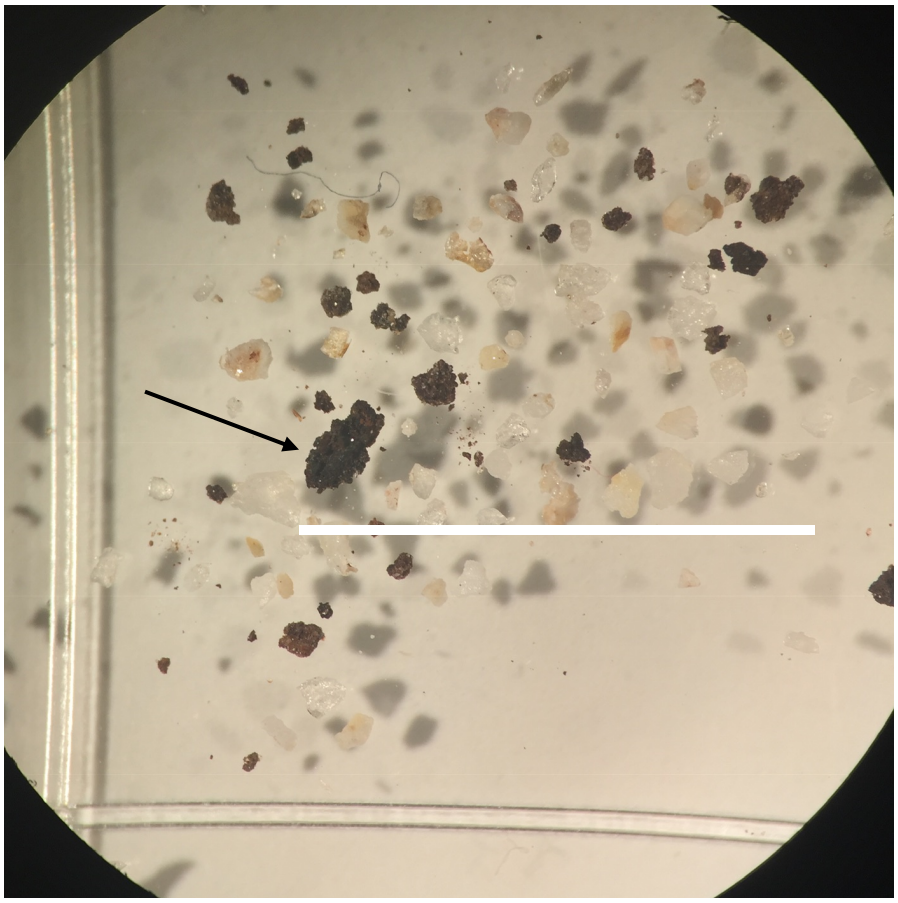

Figure 3: Good example of charcoal grains mixed with quartz and mica. The arrow points to a particularly large grain. The white bar indicates a length of 1 cm. The charcoal shown here is most likely a burned wood grain.

Age Model Creation and Data Analysis

In order to construct an age model, carbon dates were determined using material from the cores. For the purposes of carbon dating, large visible charcoal grains were recovered either directly from the core or from samples after the sieve process where no large grains were visible. When possible, large grains directly from the core were preferred in order to minimize possible contamination during the retrieval process. Samples were taken at regular intervals down the core and then sealed and shipped to an affiliated carbon dating lab at the University of Georgia. This lab uses standard carbon dating techniques and reports an age of the material (Vogel et al., 1984). Carbon dates were calibrated using the standard northern hemisphere calibration curve (Reimer et al., 2013). These dates are then input into the BACON age model which is constructed using R statistical software (Blaauw, 2010). This model uses Bayesian statistics to generate an age-depth model. This age model and the charcoal counts are then input into a modified version of the CharAnalysis software package via MatLab (Higuera et al., 2007). The CharAnalysis software uses Bayesian statistics to establish a background charcoal deposition rate and then records peaks above this background rate as discrete fire events. For this analysis, just the total (both sieves) charcoal count was used. The software is configured to use a 1,000-year

window around every point for the background calculation to account for long term changes. The software was modified from its default code for this project to count adjacent peaks as discrete events to account for the coarser resolution of a meadow environment.

Results

Core Descriptions

The oldest core (DLM14) was very difficult to drill due to dry, rocky soil and the use of the Livingston drill which is designed to drill soft lake sediments. Due to this difficult drilling process, much of the core, especially the top several sections, was heavily fractured during extraction and contains significant warping. For this reason, each section retrieved was described individually by the drive in which they were recovered (Figure 4). The top section of the core (section 1A) extends from 0 to 12 cm and contains a moist organic layer with a dark brown coloration and a well sorted fine-grained texture mostly of clay. Some cross bedded features are apparent in the lower part of this section. Section 1B spans from 12 to 20 cm. It contains about 2 cm of the organic layer seen in 1A before an abrupt transition to a moderately sorted, fine grained clay with a light brown color. This section of the core is very dry and easily crumbles. Section 1C extends from 20 to 27.5 cm and contains moderately sorted clay similar to section 1B. This layer is even drier and is dominated by a clumpy texture. Some dark black charcoal grains approximately 3mm in size are present in this section. Section 1D extends from 27.5 to 38 cm. The first 8 cm of this section consist of highly warped and fractured unconsolidated sediment. This sediment is very dry with no cohesion and consists of moderately sorted clay with a light brown color. Section 1E extends from 38 to 49 cm. This section signifies a rapid change to a very dark brown, well sorted clay. This section contains moderate moisture and includes some small charcoal grains. Section 1F extends from 49 to 63 cm. The top 5 cm of this section continue the very dark brown texture from 1E but with poorer sorting and some light grey gravel grains. Halfway through this section, there is an abrupt shift into a moist, light grey clay that quickly grades into very poorly sorted gravel consisting of grey colored clay and quartz grains. Section 1G extends from 63 to 77.5 cm and continues the same very poorly sorted gravel from 1F for the first 10cm. It then quickly grades into light brown sand and then very well sorted light brown mud. There are a few macroscale charcoal grains visible near the bottom of this section.

Below section 1F, the core record is more continuous and exhibits regular deposition indicative of a lake environment. Section 2A extends from 77.5 to 93 cm. The first 4cm of this section consist of very moist, well sorted, dark brown clay. Past 4cm, this clay abruptly grades into a similar well sorted light brown clay. Section 2B extends from 93 to 117 cm. This section is very moist and continuous. It starts with light brown clay seen in 2A and then slowly transitions to a very dark brown, well sorted clay. About 15 cm into the section, there is an abrupt appearance of abundant macroscale charcoal grains. Section 2C extends from 117 to 134.5 cm. This section contains the same fine-grained, dark brown clay as 2B for the first 4 cm before rapidly grading into a light brown clay and then abruptly returning to the same dark brown clay 11 cm into the section. The final 1 cm of this section contains very poorly sorted grey quartz gravel. There is very large (about 1 cm across) chunks of charcoal present in this section at approximately 9cm into the section.

The final section of DLM14 was extracted as a single continuous section (section 3A). The section extends from 134.5 to 183 cm. The top 14 cm of this section contains very moist, dark

brown, fine-grained clay. Past the 14 cm point, the section slowly grades into moderately sorted quartz gravel and light brown clay. This sediment extends to about 24 cm where there is an abrupt transition back to dark brown, well sorted clay. At 28 cm, there is abundant macroscale charcoal. At 38 cm, the clay quickly grades into very poorly sorted quartz gravel before switching back to very dark brown, very moist clay at 42 cm. This section slowly narrows to an end at 48 cm where bedrock was reached, and the core terminates.

One year later, core DLM15 was drilled at the same location as core DLM14 but with revised drilling techniques that allowed for the extraction of a more continuous record with significantly less warping. DLM15 extends for 1.8 m in length (Figure 5). The first 20 cm of the core contains a moderately moist organic layer with many plant roots. This section starts with a dark brown color slowly grading into light brown. It is mostly well sorted clay with sparse quartz gravel grains. There is a thin (1 cm) quartz gravel lenses at 20 cm followed by moderately sorted light brown clay. This clay is interspersed with discrete quartz gravel lenses with irregular thicknesses around the circumference of the core. This section continues to 45 cm where it abruptly transitions into a very coarse, poorly sorted quartz gravel lens. This gravel is unconsolidated and appears to extend to about 53 cm. Below 53 cm, there is a dark brown layer with well sorted clay until about 65 cm. Below 65 cm there is an abrupt transition to well sorted grey-brown clay that exhibits well preserved layering. This section contains several large, macroscale charcoal deposits at 81 cm and 88 cm. The well layered section ends at 90 cm where there is a clear transition to a light grey clay with less apparent charcoal. This grey clay grades back into a dark brown clay at 99 cm with a gravel lens at 95cm. Below 99cm there is some clear warping but also several areas of well-preserved layering. Macroscale charcoal about 0.5 cm in size is well represented especially around 65 cm. This section grades into a short, very dark brown clay layer between 121 cm and 125 cm before rapidly transitioning into a layer of poorly sorted, grey quartz sand. This sand gradually transitions back into a very dark brown clay layer by 131 cm with visible charcoal between 136 and 138 cm. Below this layer is an extensive gravel deposit of poorly sorted quartz gravel between 139 and 155 cm. There is a thin layer of charcoal and clay within this gravel at 151 cm. Between 155 cm and 165 cm, the core slowly transitions from a mix of dark brown clay and quartz gravel to a sandy clay. Below 165cm, there is a dark brown, moderately sorted sandy clay with a more fine-grain, dark brown clay layer between 177 and 179 cm which exhibits some evidence of charcoal. The core abruptly ends with a small quartz sand layer above bedrock at 182 cm.

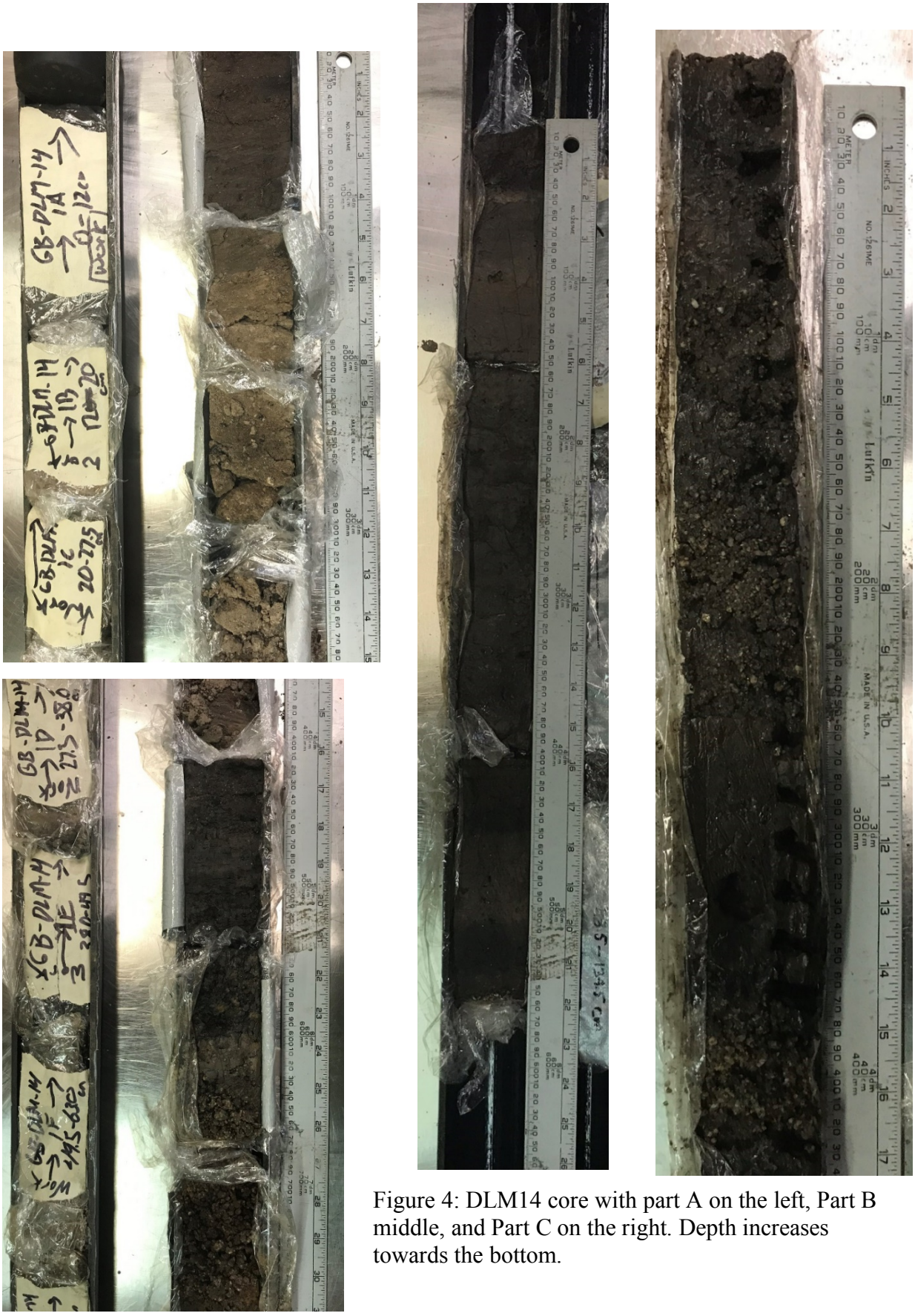

Figure 4: DLM14 core with part A on the left, Part B middle, and Part C on the right. Depth increases towards the bottom.

Figure 5: DLM15 core with increasing depth from the top left to the bottom right.

Retrieval of both SFB and SBC cores benefited from the new coring technique first used in the summer of 2018. The fully custom drilling rig allowed for both cores to be extracted as single, continuous units with minimal warping or deformation (Figure 6). Core SFB is approximately 58 cm long. The top 5 cm of the core contain large roots and wood pieces. This section represents a productive organic layer made up of peat moss. Below 5 cm, the core slowly grades into increasingly dark brown, moist clay with occasional tree roots throughout the top section. The top section also contains some areas of sand irregularly mixed into the clay. There is a significant organic content of both live and decomposing matter throughout the upper core to at least 28 cm. Below this point, roots become sparser. The clay sand mixture continuous until around 35 cm where the core transitions to a better sorted and more compacted black clay. This section contains several visible macroscale charcoal grains. Between 46 and 49 cm, there is a light gray layer of unconsolidated silt and sand. This quickly transition back to black clay with occasional areas of sandy clay until the core terminates at 56 cm.

Core SBC is slightly longer, 76 cm in length. Like core SFB, it starts with a deep organic layer of peat for about 3cm. This quickly gives way to a layer of very dark brown clay with a high organic content and many roots. There are also some buried seeds visible in the soil. The layer contains mostly well sorted clay with only occasional quartz gravel grains. This organic rich layer ends around 28 cm where it transitions into moderately sorted black clay with some quartz gravel. The layer is very moist and contains some visible macroscale charcoal. This section slowly transitions to a layer of moderately sorted grey quartz sand and gravel at 44 cm. This section continues to about 54 cm where an apparent charcoal layer demarcated the shift into a brown layer of moderately sorted clay and gravel. This clay gravel mix is very moist and continues to the end of the core at 76 cm.

Carbon Dates

Several radiocarbon dates were obtained from the cores and these samples are summarized in Table 1. Initially, only 3 samples from core DLM14 were dated given the discontinuous nature of the overall core. Several more dates were made from core DLM15. The two modern dates were removed due to very high likelihood of either contamination or accidental use of modern organic material. All other dates were kept for use in age modeling. Additional dates from core SFB and core SBC are currently pending results.

Table 1. Carbon dates					
Core	Depth (cm)	$\delta\ ^{13}C$ ($^{0}/_{00}$)	^{14}C age years BP	Date Error (+/-)	Calibrated years BP
DLM14	13	-21.4	1090	25	975
DLM14	77	-24.9	5290	30	6005
DLM14	131.5	-23.5	6710	30	7580
DLM15	10	-24.6	4450	20	5050
DLM15	14.5	-24.71	3740	20	4135
DLM15	26.5	-24.88	3450	40	3695
DLM15	30	-24.12	3590	40	3890
DLM15	39.5	-23.99	4710	30	5465
DLM15	40	-23.05	940	20	830
DLM15	61	-24.18	5010	25	5740
DLM15	65	-29.02	0	N/A	N/A
DLM15	88.5	-23.40	6180	30	7030
DLM15	104.1	-23.00	6830	35	7670
DLM15	139.3	-23.8	7430	30	8210
DLM15	164.8	-20	8110	30	9020
SFB	55.5	-24.85	7720	30	8520
SBC	60	-27.15	1300	25	1270

Figure 6: SBC core on the left and the SFB core on the right. Depth increases towards the bottom. Notice the overall coarser and less well sorted nature of SBC relative to SFB.

Age-Depth Model

While only three dates were determined for DLM14, they were chronological with depth, so a simple straight line was used to form a rudimentary age model between the two older dates. This line was only used to date the continuous middle section of the core and was not extrapolated beyond the age of these two dates. The youngest date lies within a discontinuous section of the core. Due to its discontinuous nature and lack of further dates, this top section was deemed too uncertain to model with current data. With the 12 dates determined for core DLM15, BACON age modeling software was used to create a more robust model for that core (Figure 7). The model performs well for the mostly continuous middle section of the core. The upper section of the core features a more complex order of dates. Due to an apparent age reversal, all dates above 40 cm were excluded from further analysis. Similarly, due to the presence of several gravel lenses and weak age model support, all section of the core below 140 cm were also excluded from further analysis. The continuous middle section of the core, however, provided a robust age model similar to the middle section of DLM 14.

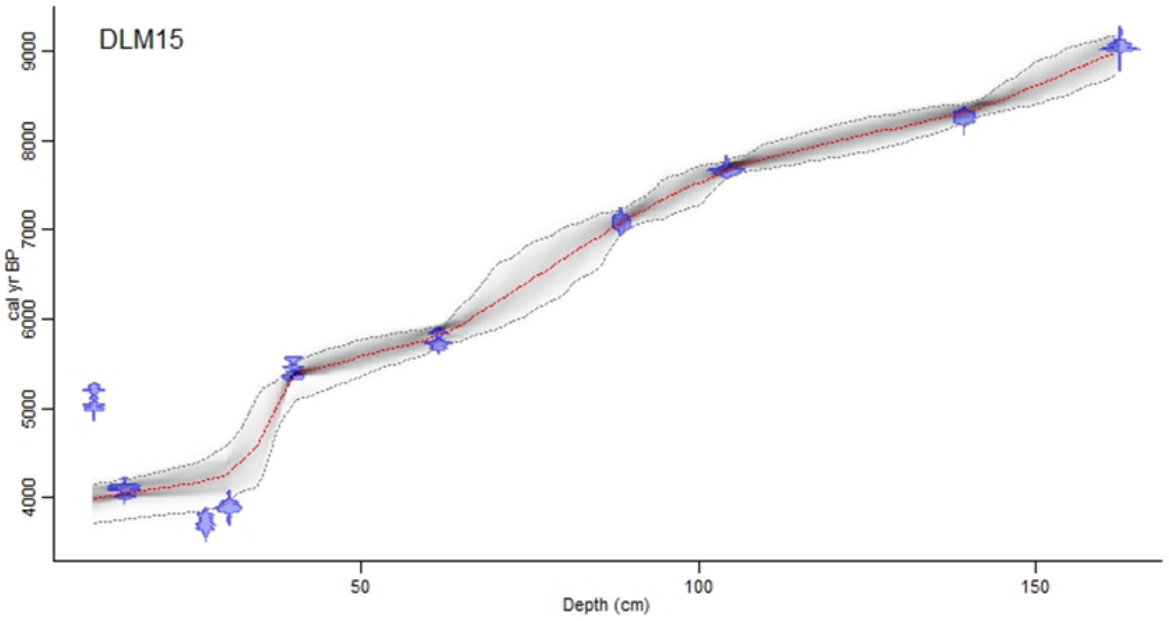

Figure 7: Constructed age model for DLM15 with depth. The shaded grey area provides a visual representation of the confidence for each extrapolated section.

Charcoal Counts

The charcoal counts from DLM14 and DLM15 are displayed below for each sieve size (Figure 8). The sieve sizes usually follow together with 125 µm exhibiting a higher amplitude. The charcoal tends to show an episodic behavior with both rapid increases and declines. Holes in the timeline represent sections of core that were lost during drilling. After 63 cm, the core DLM15 has a very sharp and rapid increase in charcoal deposition. Core DLM14 exhibits a similar overall increase in charcoal near the top of the core though its change is not as large, and the values do not remain as consistently elevated after the shift.

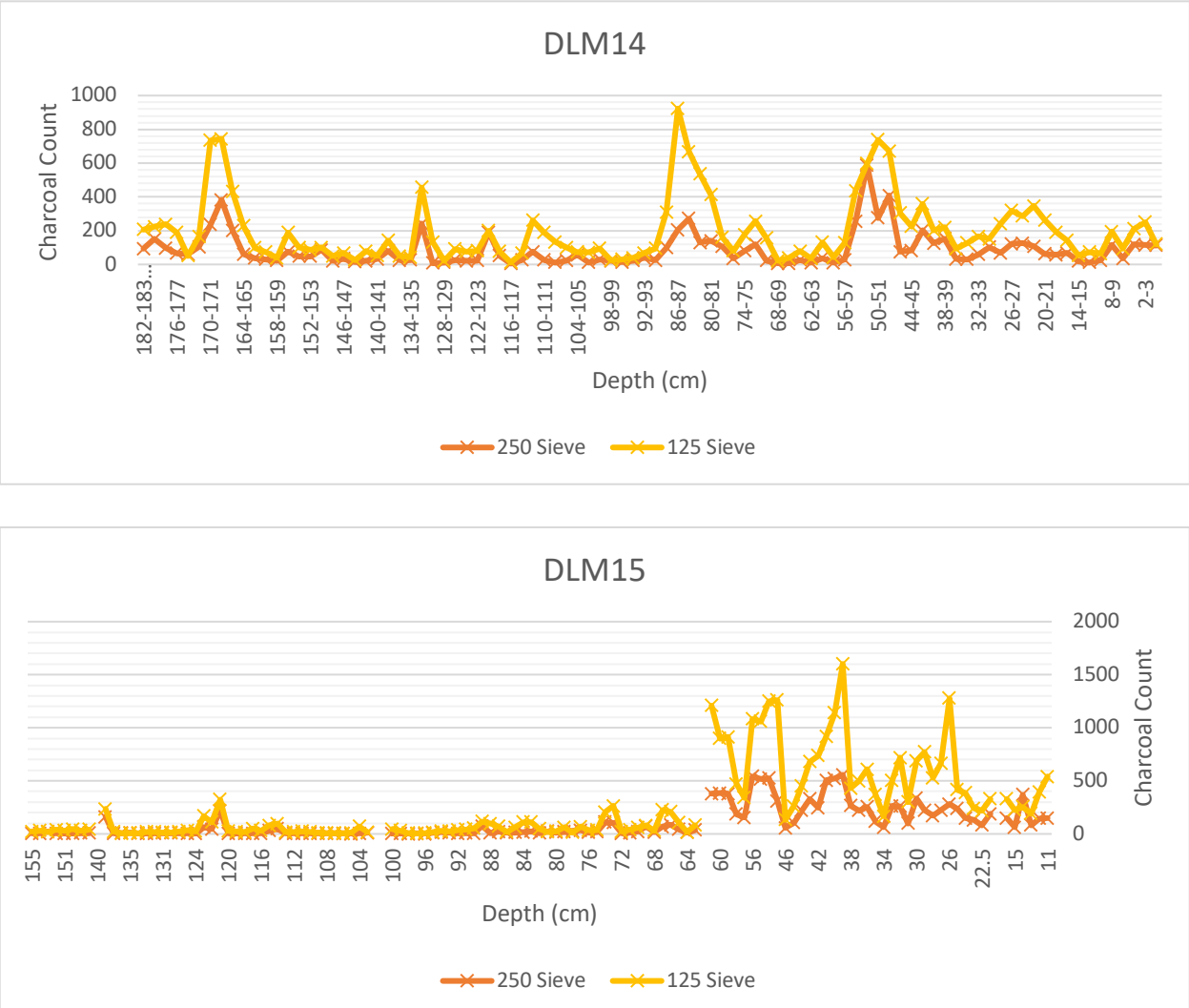

Figure 8: Charcoal counts for the DLM14 and DLM15 cores. DLM14 was sampled at half the resolution (every 2 cm rather than 1 cm) of DLM15.

CharAnalysis

The CharAnalysis peak identification software was run for the paired age models and charcoal counts for cores DLM15 and DLM14. Charcoal counts were fit to the calculated age model (Figure 9). Both cores exhibit a very strong increase in charcoal deposition in younger sections of the core. Figure 10 shows the extrapolated fire frequency calculated by using peak identification from the charcoal counts. The fire return interval is sensitive to fire identified within a 500-year interval of each point in time. Results from DLM14 show a clear shift in fire return interval about 6,400 years ago. DLM15's much more extensive charcoal record shows a similar strong environmental shift around this time. The overall shape agrees between both cores, but the timing does not. The overall shape of the calculated fire return interval is also similar between the cores, but DLM14 has a lower fire frequency than DLM15.

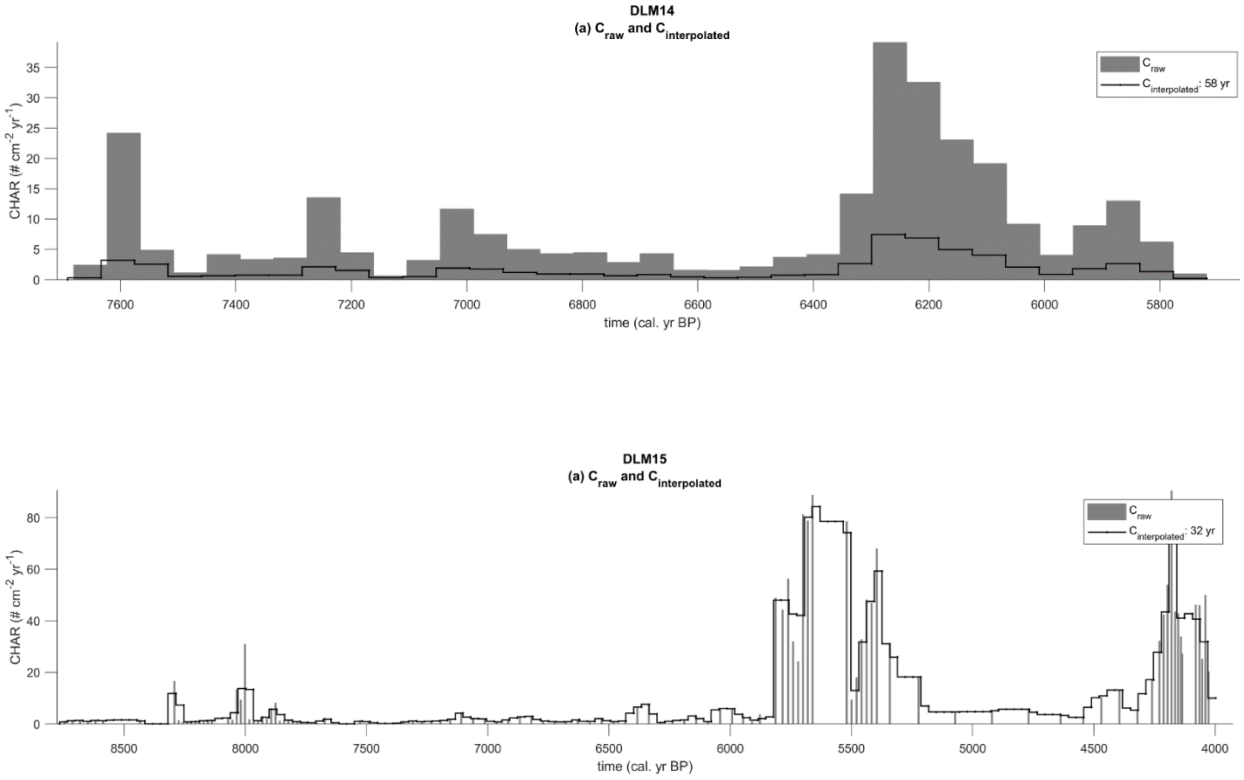

Figure 9: Charcoal counts extrapolated over time using the age model. The data is reported as a deposition rate.

DLM14 DLM15

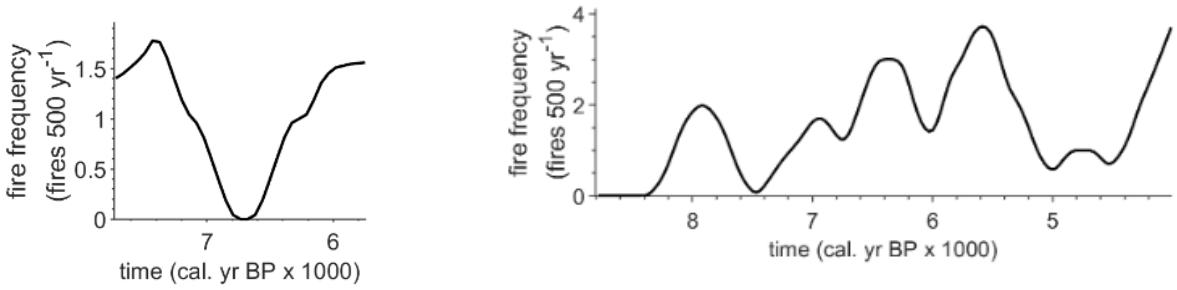

Figure 10: Calculated fire frequency for DLM14 on the left and DLM15 on the right. Both show a generally active regime in the past followed by a dip in fire activity and then a second rise but with an offset timing between the two.

Discussion

7,600 Calibrated Years Before Present and Older

Neither DLM14 or DLM15 is dated with high accuracy prior to 7,800 years before present (YBP), and SFB and SBC are too young to cover this time range. Furthermore, the depositional environment prior to 7,800 years BP appears highly variable with thick gravel lenses and inconsistent grain size. These caveats in mind, there is still some information regarding fire history that can be inferred from these sections. Broadly speaking, fire events seem relatively small and sporadic in nature, with an estimated fire frequency of two fires per thousand years. Approximately 8,200 to 7,600 years ago there is a period of elevated fire activity seen in DLM15 with a similar peak seen at a slightly later time in DLM14. Other eastern Great Basin paleorecords from this period are sparse but there is evidence in sediment cores from Blue Lake in western Utah that the Great Basin was relatively warm and dry during the mid-Holocene with variable summer precipitation (Louderback et al., 2010). Speleothem records from Lehman caves within the park also indicate an abrupt climate drying and warming event initiating around 8,200 YBP (Steponaitis et al., 2015). This climate shift likely helped trigger an increase in fire activity.

Overall charcoal behavior in this older section of the cores appears more sporadic with more variable charcoal peaks and larger disagreement between DLM15 and DLM14 than in younger portions. The low sampling resolution of DLM14 and the age model uncertainty associated with both cores can explain some of this variation. Vegetation assemblage may play an important role. Pollen analysis covering this period suggests that the region had greater coverage of grasses such as ragweed and sage and lesser coverage by conifer trees than seen today (Mensing et al., 2004). Sage and ragweed are both fire prone species that dry and burn on annual time scales (Miller et al., 2013). Many of these local burning events are likely to have generated very fine charcoal grains that are not well preserved within the sediment core, meaning only intense fires burning sparse tree cover or intense grass fire directly over the core location but are also likely to be preserved (Ohlson & Tryterud, 2000; Crawford & Belcher, 2014). This behavior may help explain the lower relative magnitude of charcoal peaks in the older sections of the core compared to the new sections. There may also be a local bias due to the site location. Since DLM comprises a local depression, it is likely to remain wetter than its surrounding, perhaps suppressing fire within the immediate vicinity, especially of grass-based fuels.

7,600 to 5,400 Calibrated Years Before Present

The 7,600 to 5,500 YBP time period covers the middle section of cores DLM14 and DLM15. Early carbon date results indicate that this period is likely also covered by SFB, but the analysis for SFB was not completed in time for this thesis. The middle section of these cores is well dated with a continuous stratigraphy giving confidence to the analysis. The numerical analysis via CharAnalysis covers this period for both cores. The older part of this section from 7,600 to 6,300 YBP is marked by a relatively quiet fire regime with a very long return interval of one fire every 500 years compared to the modern interval of one fire every 100 years. Fire frequency in general exhibits an increasing trend over this period. There is a noticeable clustering of fires about 7,000 YBP in both DLM cores. The century previous to this section was unusually wet according to speleothem records from Lehman caves, which may have allowed vegetation to

buildup (Steponaitis et al., 2015). Upon return to dryer conditions, the vegetation could have served to generate fires observed in the core. Between 7,000 BP and 6,300 YBP, there is disagreement among climate records within the Great Basin (Wahl et al., 2015). Speleothem records from Lehman cave indicate intensifying drought during this period while evidence from Stella Lake within the park suggests the period to be cool and wet (Reinemann et al., 2009). Disagreement between records within the Park may be explained by some kind of elevation gradient interaction; Stella Lake is a much higher elevation than Leheman caves. Models utilizing paleo-oceanographic information from the Gulf of California indicate a shift of the North American Monsoon (NAM) initiating around 7,000 YBP (Barron et al., 2012). This shift likely pushed the NAM westward into eastern Nevada. Great Basin National Park lies along the edge of the NAM during this time, so summer precipitation was probably highly variable and also likely to be elevation dependent due to the Park's peripheral location within the NAM. The monsoon's partial coverage of the Great Basin in this period also helps explain the large paleorecord disagreement on a regional scale. DLM lies at an elevation between the two other paleoclimate sites in the park, so DLM likely received a rainfall amount somewhere between the wet conditions seen at Stella Lake and the very dry conditions seen at Lehman cave. The relatively quiet but irregular fire activity between 7,000 and 6,300 YBP suggests an overall wet but variable environment at DLM.

Moving forward in time, both DLM cores show an abrupt increase in fire activity around 6,000 YBP, peaking at a fire return interval of 3.5 per 500 years. The timing of this shift between DLM14 and DLM15, however, is inconsistent. DLM14 records a shift around 6,300 YBP while DLM15 records a similar shift at 5,800 YBP. The peaks appear very distinct in the pure charcoal counts of both cores with very similar double-peaked forms, so the charcoal signatures are potentially the same event. Many factors could explain this discrepancy including uncertainty in age-model construction and errors in the carbon dates. Due to its continuous nature, higher age-model confidence, and higher sampling resolution, the DLM15 timing is favored here over DLM14. The abrupt 5,800 years BP timing aligns well with a number of other paleoclimate records. One of these is the chironomid-based analysis within the park along with records from Pyramid lake and speleothems all indicate a maximum of warm temperatures around this time period (Reinemann et al., 2009). These warm temperatures aligned with a climate that had been drying over the prior 1,000 years, likely contributing fuel for large, violent wildfires in the area. It should be noted that although the climate had been drying for some time before this shift in fire regime, the shift itself happens in much closer timing to temperature increases than to precipitation. This connection may suggest that fire regimes in Great Basin are more closely linked to temperature than precipitation. Another paleoclimate record supporting the charcoal analysis herein is the pollen analysis in the region which suggests that leading up to the 6,000 YBP shift, tree lines likely shifted lower, to near-modern elevations, bringing trees to the elevation of Dead Lake meadow (Louderback et al., 2010). Under drying conditions, these trees could create much more intense burning than grass alone, helping explain the very large magnitude of the charcoal peaks observed during this time period. The Lehman cave speleothem record alone records evidence of a local, extreme peak in precipitation approximately 5,600 YBP, possibly associated with the North American Monsoon (Barron et al., 2012). This short burst of moisture may create the double peaked nature in fire activity observed in the dire record. The speleothem records also indicate that warm, dry conditions continued to intensify until about 5,400 YBP, which aligns well with the fire frequency peak modeled from DLM15 at that time

(Steponaitis et al., 2015). Support for drought in this period comes from a variety of other records, including archeological records indicating drought stress on native American societies (Louderback et al., 2010). Subsequently, however, fire activity appears to slow even though other records indicate that the climate remains warm and dry for a few hundred years before cooling again (Reinemann, et al. 2009). A fire-mediated retreat of the tree line could help explain the difference in charcoal magnitude here as more drought resistant vegetation return with charcoal that is more rarely preserved (Madsen et al., 2001). It should be emphasized that high variability persists in other paleoclimate records throughout the Great Basin region between 7,600 and 5,400 YBP (Wahl et al., 2015). Due to this variability, very local paleoclimate records were emphasized in this analysis.

5,400 Calibrated Years Before Present and Younger

The younger sections of both DLM14 and DLM15 are problematic. This time period spans sections of each core that are discontinuous and contain many gravel lenses. Dates from DLM15 in particular show an apparent age reversal in this period. This reversal, along with the more abundant coarser and poorly sorted sediments, indicates an increase in the power of the depositional environment that is conceivably depositing re-mobilized charcoal that has been eroded from elsewhere in the basin (Patterson et al., 1987). For this reason, the charcoal records of these cores younger than 5,400 years are likely highly unreliable and unsuitable for interpretation. Nonetheless, an overall higher-powered depositional environment implies some increase in precipitation. Indeed, there is evidence from the Lehman cave speleothems that precipitation began increasing by 5,000 YBP (Steponaitis et al., 2015). On a regional scale, many records agree that a cooler, wetter climate began to form around 5,000 YBP (Wahl et al., 2015). Conveniently, the only other charcoal analysis done in the Great Basin region starts at 5,500 YBP. Conducted in 2006, this other charcoal analysis was located in central Nevada and focused on low elevation grass fire behavior (Mensing et al., 2006). DLM represents a very different environment than the central Nevada study, so comparisons should be made with caution. Nevertheless, the central Nevada study also showed elevated fire activity around 5,500 YBP and a wet environment forming and persisting for several hundred years afterward. Overall, it is clear that the local climate was getting wetter at this time, likely leading to a drop in fire activity. Precipitation rates were likely higher earlier in the core record, so why this period saw such strong deposition is unclear and is likely related to very local changes in the geomorphology. This time period is likely also covered by the SFB core, but the younger parts of that core contain very large amounts of peat that likely preclude confident charcoal analysis.

Recommendations for Future Work

This thesis suggests many promising avenues for future work. First, completion of the charcoal analysis from both of the 2018 cores (SFB and SBC) is a top priority. These cores are already being counted and dates to construct an age model have already been ordered, so they should provide a complementary analysis very soon. These cores will provide a local basis of comparison for both DLM cores. In addition, a pollen analysis done within the park would provide solid connection between possible changes in ecology and fire within the park. Additional cores should also be extracted within the park to broaden coverage for more time periods, especially those with sporadic deposition. Broader geographic diversity in the core sites is also required in order to test that fire frequency was regionally consistent throughout the park as a whole. On a larger scale, the whole Great Basin region would benefit from further charcoal analysis in order to better understand the geographic variation in fire response.

References Cited

Barron, J. A., Metcalfe, S. E., & Addison, J. A. (2012). Response of the North American monsoon to regional changes in ocean surface temperature. *Paleoceanography*, *27*(3). https://doi.org/10.1029/2011pa002235

Blaauw, M., 2010. Methods and code for 'classical' age-modelling of radiocarbon sequences. Quaternary Geochronology 5, 512-518

Crawford, A. J., & Belcher, C. M. (2014). Charcoal Morphometry for Paleoecological Analysis: The Effects of Fuel Type and Transportation on Morphological Parameters. *Applications in Plant Sciences*, *2*(8), 1400004. https://doi.org/10.3732/apps.1400004

Higuera, P. E., Brubaker, L. B., Anderson, P. M., Hu, F. S., & Brown, T. A. (2009). Vegetation mediated the impacts of postglacial climate change on fire regimes in the south-central Brooks Range, Alaska. *Ecological Monographs*, *79*(2), 201–219. https://doi.org/10.1890/07-2019.1

Kilpatrick, M., Biondi, F., Strachan, S., & Sibold, J. S. (2013). Fire history of mixed conifer ecosystems in the Great Basin/Mojave Deserts transition zone, Nevada, USA. *Trees*, *27*(6), 1789–1803. https://doi.org/10.1007/s00468-013-0924-7

Louderback, L. A., Grayson, D. K., & Llobera, M. (2010). Middle-Holocene climates and human population densities in the Great Basin, western USA. *The Holocene*, *21*(2), 366–373. https://doi.org/10.1177/0959683610374888

Madsen, D., Rhode, D., Grayson, D., Broughton, J., Livingston, S., Hunt, J., Quade, J., Schmitt, D.N., & Shaver, M. (2001). Late Quaternary environmental change in the Bonneville basin, western USA. *Palaeogeography, Palaeoclimatology, Palaeoecology*, *167*(3-4), 243–271. https://doi.org/10.1016/s0031-0182(00)00240-6

Mensing, S. A., Benson, L. V., Kashgarian, M., & Lund, S. (2004). A Holocene pollen record of persistent droughts from Pyramid Lake, Nevada, USA. *Quaternary Research*, *62*(01), 29–38. https://doi.org/10.1016/j.yqres.2004.04.002

Mensing, S. A., Livingston, S., & Barker, P. (2006). Long-Term Fire History in Great Basin Sagebrush Reconstructed from Macroscopic Charcoal in Spring Sediments, Newark Valley, Nevada. *Western North American Naturalist*, *68*(1), 64–77. https://doi.org/10.3398/1527-0904(2006)66

Miller, R. F., Chambers, J. C., Pyke, D. A., Pierson, F. B., & Williams, C. J. (2013). *A Review of Fire Effects on Vegetation and Soils in the Great Basin Region: Response and Ecological Site Characteristics* (RMRS-GTR-308). Retrieved from http://sagestep.org/pdfs/rmrs_gtr308.pdf

Ohlson, M., & Tryterud, E. (2000). Interpretation of the charcoal record in forest soils: forest fires and their production and deposition of macroscopic charcoal. *The Holocene*, *10*(4), 519–525. Retrieved from https://pdfs.semanticscholar.org/3c9e/56fe6b474289ffc2af88646e7c167b8dcc33.pdf

Paterson III, W. A., Edwards, K. J., & Maguire, D. J. (1987). Microscopic Charcoal as a Fossil Indicator of Fire. *Quaternary Science Review*, *6*, 3–23. Retrieved from https://www.umass.edu/nebarrensfuels/publications/pdfs/wap_charcoal_fire_1987.pdf

Reimer, P. J. et al. (2013). IntCal13 and Marine13 Radiocarbon Age Calibration Curves 0–50,000 Years cal BP. *Radiocarbon*, *55*(04), 1869–1887. https://doi.org/10.2458/azu_js_rc.55.16947

Reinemann, S. A., Porinchu, D. F., Bloom, A. M., Mark, B. G., & Box, J. E. (2009). A multi-proxy paleolimnological reconstruction of Holocene climate conditions in the Great Basin, United States. *Quaternary Research*, *72*(03), 347–358. https://doi.org/10.1016/j.yqres.2009.06.003

Steponaitis, E., Andrews, A., McGee, D., Quade, J., Hsieh, Y., Broecker, W. S., . . . Cheng, H. (2015). Mid-Holocene drying of the U.S. Great Basin recorded in Nevada speleothems. *Quaternary Science Reviews*, *127*, 174–185. https://doi.org/10.1016/j.quascirev.2015.04.011

Vogel, J., Southon, J., Nelson, D., & Brown, T. (1984). Performance of catalytically condensed carbon for use in accelerator mass spectrometry. Nuclear Instruments and Methods in Physics Research Section B: Beam Interactions with Materials and Atoms, 5(2), 289–293. https://doi.org/10.1016/0168-583x(84)90529-9

Wahl, D., Starratt, S., Anderson, L., Kusler, J., Fuller, C., Addison, J., & Wan, E. (2015). Holocene environmental changes inferred from biological and sedimentological proxies in a high elevation Great Basin lake in the northern Ruby Mountains, Nevada, USA. *Quaternary International*, *387*, 87–98. https://doi.org/10.1016/j.quaint.2015.03.026

Whitlock, C., & Larson, C. P. S. (2001). Charcoal as a Fire Proxy. In C. Whitlock, & C. P. S. Larsen (Eds.), *Tracking Environmental Change Using Lake Sediments: Terrestrial, Algal, and Siliceous Indicators* (pp. 75–97). https://doi.org/10.1007/0-306-47668-1_5

Appendix

DLM14 Charcoal Counts		
Depth (Cm)	250µm	125µm
182-183	114	690
182-183	84	214
182-183	79	198
182-183 (Averaged)	92.33333	206
180-181	151	224
178-179	97	238
176-177	66	189
174-175	61	51
172-173	104	165
170-171	236	735
168-169	382	744
166-167	202	431
164-165	61	228
162-163	37	98
160-161	29	73
158-159	22	39
156-157	75	188
154-155	48	101
152-153	48	86
150-151	85	101
148-149	20	50
146-147	33	68
144-145	15	26
142-143	20	78
140-141	31	51
138-139	80	142
136-137	24	50
134-135	27	42
132-133	241	456
130-131	8	132
128-129	12	20
126-127	27	92
124-125	20	76
122-123	22	81
120-121	190	200

118-119	**51**	**77**
116-117	**5**	**12**
114-115	**27**	**65**
112-113	**75**	**261**
110-111	**27**	**188**
108-109	**12**	**132**
106-107	**23**	**101**
104-105	**56**	**73**
102-103	**11**	**71**
100-101	**29**	**95**
98-99	**21**	**24**
96-97	**14**	**30**
94-95	**22**	**39**
92-93	**39**	**68**
90-91	**25**	**94**
88-89	**98**	**310**
86-87	**205**	**923**
84-85	**272**	**667**
82-83	**129**	**536**
80-81	**140**	**412**
78-79	**105**	**159**
76-77	**35**	**81**
74-75	**81**	**176**
72-73	**118**	**256**
70-71	**22**	**157**
68-69	**7**	**21**
66-67	**6**	**39**
64-65	**26**	**78**
62-63	**9**	**36**
60-61	**37**	**131**
58-59	**10**	**42**
56-57	**28**	**127**
54-55	**254**	**437**
52-53	**586**	**598**
50-51	**275**	**739**
48-49	**407**	**671**
46-47	**75**	**304**
44-45	**83**	**225**
42-43	**202**	**359**
40-41	**125**	**202**
38-39	**152**	**219**

36-37	31	93
34-35	30	128
32-33	58	166
30-31	102	150
28-29	67	242
26-27	122	318
24-25	126	287
22-23	108	346
20-21	62	263
18-19	56	190
16-17	67	142
14-15	18	53
12-13	12	73
10-11	25	64
8-9	114	194
6-7	35	93
4-5	118	210
2-3	114	250
0-1	112	121

DLM15 Charcoal Counts		
250µm	125µm	Depth (cm)
148	539	11
144	392	12
83	190	13
369	255	14
63	226	15
147	328	16
189	328	17.5
83	216	22.5
132	240	23
147	387	24
236	415	25
280	1277	26
222	666	27
172	527	28
223	772	29
336	689	30
99	302	31
261	718	32

262	502	33
63	166	34
117	369	35
255	609	36
219	499	37
265	431	38
557	1601	39
521	1140	40
505	920	41
246	737	42
330	680	43
219	452	44
106	262	45
56	135	46
309	1261	47
524	1250	54
515	1060	55
541	1083	56
155	341	57
185	469	58
379	914	59
384	898	60
377	1209	61
		62
36	81	63
13	17	64
41	105	65
85	209	66
69	227	67
15	30	68
70	80	69
21	59	70
11	40	71
5	23	72
104	263	73
110	207	74
19	36	75
12	32	76
32	67	77
27	12	78
19	61	79

12	24	80
24	19	81
8	48	82
26	112	83
17	112	84
12	63	85
10	20	86
22	70	87
6	96	88
73	117	89
5	53	90
6	42	91
4	36	92
9	26	93
16	27	94
9	16	95
0	7	96
3	2	97
0	8	98
2	29	99
2	46	100
		101
		102
9	15	103
5	70	104
0	9	105
3	3	106
4	8	107
4	7	108
3	10	109
3	18	110
3	25	111
5	20	112
3	17	113
49	97	114
30	80	115
5	31	116
3	50	117
4	16	118
2	22	119
3	28	120

218	323	121
46	112	122
65	169	123
1	26	124
4	34	125
6	22	129
6	13	130
6	14	131
3	19	132
2	20	133
1	8	134
9	8	135
8	3	136
3	21	137
160	234	138
		140
6	42	144
8	29	149
2	45	150
1	29	151
5	38	152
21	20	153
4	30	154
5	22	155